Kovove Mater. 50 2012 115–123
DOI: 10.4149/km_2012_2_115

The effective boron diffusion coefficient in Fe_2B layers with the presence of chemical stresses

M. Ortiz-Domínguez[1], I. Campos-Silva[1]*, G. Ares de Parga[2], J. Martínez-Trinidad[1], M. Y. Jiménez-Reyes[1], G. Rodríguez-Castro[1], E. Hernández-Sánchez[1]

[1]*National Polytechnic Institute, IPN, Surface Engineering Group, SEPI-ESIME, U. P. Adolfo López Mateos, Zacatenco, Mexico D. F., 07738, Mexico*
[2]*National Polytechnic Institute, IPN, SEPI-ESFM, U.P. Adolfo López Mateos, Zacatenco, Mexico D. F., 07738, Mexico*

Received 5 September 2011, received in revised form 27 September 2011, accepted 29 September 2011

Abstract

In this study the effective boron diffusion coefficient (D_{eff}) was estimated in the Fe_2B layer in the presence of chemical stresses. Boride layers were created at the surface of AISI 1018 borided steels by the paste boriding process, in which a 4-mm-thick layer of boron carbide paste was applied to the material surface. The treatment was carried out at 1123, 1173, 1223 and 1273 K with different exposure times for each temperature. The effective boron diffusion coefficients in the Fe_2B layer were estimated by combining an expression that considers the stresses in the boride layer and the flux equation. In addition, an expression to evaluate the boride layer thickness was developed, and the calculated results were compared with the experimental data and the empirical models proposed in the literature.

K e y w o r d s: boriding, growth kinetics, boride layers, effective boron diffusion coefficient, chemical stress

1. Introduction

Boriding is a thermochemical surface hardening process that diffuses boron into a well-cleaned base metal (steel) surface at a high temperature. The boriding process takes place at temperatures between 1123 and 1273 K over a period of 1 to 10 h. The resulting metallic boride provides hardness, high wear resistance, high temperature resistance and corrosion resistance [1]. Boriding of steel alloys results in the formation of either a single-phase or double-phase layer with a definite composition [2]: the outer layer is FeB (with an orthorhombic crystalline structure), and with a boron content of approximately 100.5×10^3 mol m^{-3}, and the inner layer (Fe_2B) has a tetragonal crystalline structure with a boron content of approximately 59.8×10^3 mol m^{-3}.

In addition to its selectivity, the paste-based treatment requires less manual work than the powder-pack boriding process [3]. The paste consists of B_4C and Na_3AlF_6, which is the principal activator. An inert atmosphere is necessary to enable boron diffusion. In fact, there are three important parameters that control the paste boriding process: time, temperature and the boron potential surrounding the material surface [4].

Some studies of the growth kinetics of boride layers at the surface of different ferrous alloys consider the fundamental solution of Fick's Laws in the growth of borided layers: they assume that the layers obey the parabolic growth law and that the diffusion coefficient is independent of the boron concentration at each interface [2, 4–10]. The boron diffusion coefficient obtained by these models assumes a boride surface layer that is free of chemical stresses. Chemical or diffusion-induced stresses are generated by composition inhomogeneity during mass transfer. Thus, a non-uniform stress-free deformation field can be formed that produces contraction on one side of the diffusion couple and expansion on the other. The effects of these chemical stresses also strongly depend on the possible relaxation mechanisms (e.g., Kirkendall shift, creep, dislocation slip, and bending), and on their time scale relative to the diffusion annealing time. The internal

*Corresponding author: tel: (+52) (55) 57296000 ext. 54768; fax: (+52) (55) 57296000 ext. 54589; e-mail address: icampos@ipn.mx

stress contributes to the thermodynamic potential for diffusion of atomic species ("gradient effect"), and influences the value of the diffusion coefficient. Furthermore, it leads to plastic deformation and gives rise to an elastic contribution as well. Convective transport, result of the plastic flow that is manifested as creep, dislocation glide or both, obviously relaxes the internal stress, which can lead to a feedback effect [11].

In addition, the stresses caused by a concentration with a distribution of solutes are similar to those caused by a temperature distribution (thermal stresses) in a medium and can be termed chemical stresses [12–14]. In the boriding process, compressive residual (thermal) stresses exist in the boride layer during layer growth, and these (thermal) stresses increase during cooling as a result of the volume misfit generated by the different thermal expansion coefficients of the boride layer and the substrate. Upon cooling, the substrate shrinks more than the boride layer because of its larger coefficient of linear expansion. As a consequence, a thermally induced compressive strain is imposed on the layer, attaching it to the substrate at temperatures below the boriding temperature, a process that may be aided by additional growth misfit [12]. Moreover, the magnitude and distribution of stresses depend to a considerable extent on the phase composition of the boride coating. The most favorable distribution of stresses results when the coating consists of Fe_2B alone.

In this work, the effective boron diffusion coefficient (D_{eff}) in the Fe_2B layer under chemical stress was estimated by a mathematical model that takes into account concepts from the theory of elasticity and combines them with the diffusion flux equation. The effective boron diffusion coefficient determines the speed with which the Fe_2B layer forms on the AISI 1018 steel as a function of the boriding temperature, the boron concentration profile along the Fe_2B layer, the boride incubation time, and the elastic constants of the boride layer (Young's modulus and Poisson's ratio). Moreover, an expression to determine the Fe_2B layer thickness was obtained, and its results were compared with experimental data, and empirical equations proposed in the literature.

2. The diffusion model

2.1. The mass balance equation

The model considers a system in which a solute is added to the surface of a two-phase alloy with a composition C_0. As boron is added to the surface, it is used completely in the conversion of the Fe phase to Fe_2B. There is no boron flux out of the surface layer of Fe_2B into the two-phase alloy. The boron concentration along the depth of the sample surface is illustrated in Fig. 1. The term $C^{\text{B}}_{\text{ads}}$ is the effective boron concentration (or adsorbed concentration) [10].

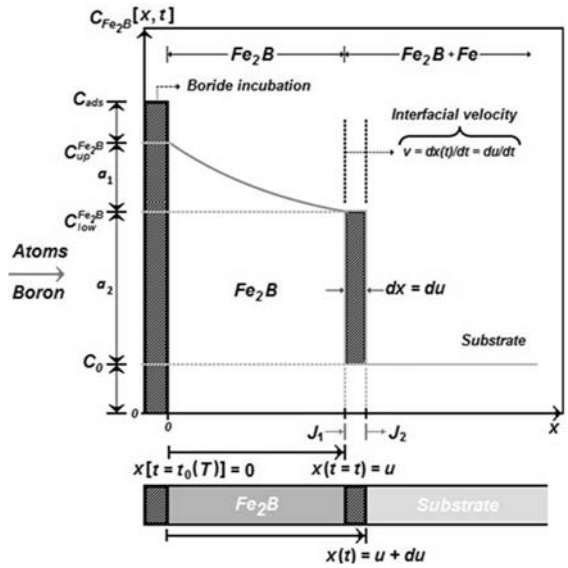

Fig. 1. Boron concentration profile in the Fe_2B layer.

Certain assumptions are considered for the diffusion model:

(i) The boron concentration $C_{\text{Fe}_2\text{B}}[x(t), t]$ in the Fe_2B layer (Fig. 1) is the solution of Fick's Second Law in a semi-infinite medium, and it depends on the position $x(t)$ and time t.

(ii) Fick's Law is valid only for dilute or ideal solutions, where

$$\left(\frac{\partial \ln \gamma}{\partial \ln C_{\text{Fe}_2\text{B}}[x(t), t]}\right)_{T,\ \sigma=\text{constant}} = 0.$$

(iii) The growth kinetics is controlled by boron diffusion in the Fe_2B layer.

(iv) The boride layer grows because of boron diffusion perpendicular to the specimen surface.

(v) Boron concentrations remain constant in the boride layer during the treatment.

(vi) The differences in specific volume per solvent atom for the Fe_2B layer are fully accounted for in the diffusion direction.

(vii) The influence of the alloying elements on the growth kinetics of the layer is not taken into account.

(viii) The Fe_2B nucleates after a certain incubation time.

(ix) The boride layer is thin compared to the sample thickness.

(x) The volume change during the phase transformation is not considered.

(xi) A uniform temperature is assumed throughout the sample.

The diffusion of boron atoms in the Fe substrate is

assumed to obey Fick's Second Law, thus:

$$\frac{\partial}{\partial t}C_{\mathrm{Fe_2B}}[x(t),t] = D_{\mathrm{Fe_2B}}\frac{\partial^2}{\partial x^2}C_{\mathrm{Fe_2B}}[x(t),t], \quad (1)$$

where $D_{\mathrm{Fe_2B}}$ denotes the boron diffusion coefficient in the Fe_2B layer in the absence of chemical stresses, and $C_{\mathrm{Fe_2B}}[x(t),t]$ is the boron concentration at depth $x(t)$, after time t and at temperature T. A general solution of Eq. (1) was given by Kirkaldy et al. [15]:

$$C_{\mathrm{Fe_2B}}[x(t),t] = A + B\,\mathrm{erf}\left(\frac{x}{\sqrt{4D_{\mathrm{Fe_2B}}t}}\right), \quad (2)$$

where $\mathrm{erf}(x/\sqrt{4D_{\mathrm{Fe_2B}}t})$ is Gauss's error function, A and B are constants that depend on the initial and boundary conditions of the diffusion problem.

Equation (2) is subject to the following initial and boundary conditions (Fig. 1):

$$C_{\mathrm{Fe_2B}}[x(t=0)=x,0] = C_0 \approx 0, \quad (3)$$

$$C_{\mathrm{Fe_2B}}\{x[t=t_0(T)]=0,t_0(T)\} = C_{\mathrm{up}}^{\mathrm{Fe_2B}},$$
$$\text{for } C_{\mathrm{ads}}^{\mathrm{B}} > 59.8\times10^3\,\mathrm{mol\,m^{-3}}, \quad (4)$$

$$C_{\mathrm{Fe_2B}}[x\,(t=t)=u,t] = C_{\mathrm{low}}^{\mathrm{Fe_2B}},$$
$$\text{for } C_{\mathrm{ads}}^{\mathrm{B}} < 59.8\times10^3\,\mathrm{mol\,m^{-3}}, \quad (5)$$
$$\text{for } 0 \le x \le u,$$

where $C_{\mathrm{up}}^{\mathrm{Fe_2B}}$ represents the upper boron concentration limit in the Fe_2B layer ($59.8\times10^3\,\mathrm{mol\,m^{-3}}$), $C_{\mathrm{low}}^{\mathrm{Fe_2B}}$ is the lower boron concentration limit in the Fe_2B layer ($59.202\times10^3\,\mathrm{mol\,m^{-3}}$), and $t_0(T)$ is the boride incubation time. Given the aforementioned conditions, and taking into account that the layer depth u is governed by the parabolic growth law $u = k_{\mathrm{Fe_2B}}[t^{1/2} - t_0^{1/2}(T)]$, where $k_{\mathrm{Fe_2B}}$ is the parabolic constant, the boron concentration profile in the Fe_2B layer is established as follows:

$$C_{\mathrm{Fe_2B}}[x(t),t] = C_{\mathrm{up}}^{\mathrm{Fe_2B}} + \quad (6)$$
$$+\frac{C_{\mathrm{low}}^{\mathrm{Fe_2B}} - C_{\mathrm{up}}^{\mathrm{Fe_2B}}}{\mathrm{erf}\left\{\dfrac{k_{\mathrm{Fe_2B}}\{1-[t_0(T)/t]^{1/2}\}}{\sqrt{4D_{\mathrm{Fe_2B}}}}\right\}}\mathrm{erf}\left(\frac{x}{\sqrt{4D_{\mathrm{Fe_2B}}t}}\right).$$

Thus, the mass balance equation is established at the Fe_2B/substrate interface [15, 16]:

$$(C_{\mathrm{low}}^{\mathrm{Fe_2B}} - \beta C_0)\left(\frac{\mathrm{d}x(t)}{\mathrm{d}t}\right)\Big|_{x(t)=u} =$$
$$-D_{\mathrm{Fe_2B}}\frac{C_{\mathrm{low}}^{\mathrm{Fe_2B}} - C_{\mathrm{up}}^{\mathrm{Fe_2B}}}{\mathrm{erf}\left\{\dfrac{k_{\mathrm{Fe_2B}}\{1-[t_0(T)/t]^{1/2}\}}{\sqrt{4D_{\mathrm{Fe_2B}}}}\right\}}\cdot \quad (7)$$
$$\cdot\frac{\partial}{\partial x}\mathrm{erf}\left(\frac{x}{\sqrt{4D_{\mathrm{Fe_2B}}t}}\right)\Big|_{x(t)=u}$$

The constant $\beta = 0.23$ represents the ratio of the specific volume to the number of solvent atoms, and it is expressed as $\beta = V_0^{\mathrm{m}}/2V_{\mathrm{Fe_2B}}^{\mathrm{m}}$, where V_0^{m} is the molar volume ($\mathrm{m^3\,mol^{-1}}$) of the substrate and $V_{\mathrm{Fe_2B}}^{\mathrm{m}}$ is the molar volume ($\mathrm{m^3\,mol^{-1}}$) of the Fe_2B layer.

Substituting Eq. (6) into Eq. (7) yields the following:

$$(C_{\mathrm{low}}^{\mathrm{Fe_2B}} - \beta C_0)k_{\mathrm{Fe_2B}} =$$
$$-2\sqrt{\frac{D_{\mathrm{Fe_2B}}}{\pi}}\frac{C_{\mathrm{low}}^{\mathrm{Fe_2B}} - C_{\mathrm{up}}^{\mathrm{Fe_2B}}}{\mathrm{erf}\left\{\dfrac{k_{\mathrm{Fe_2B}}\{1-[t_0(T)/t]^{1/2}\}}{\sqrt{4D_{\mathrm{Fe_2B}}}}\right\}}\cdot$$
$$\cdot\exp\left(-\frac{k_{\mathrm{Fe_2B}}^2\{1-[t_0(T)/t]^{1/2}\}^2}{4D_{\mathrm{Fe_2B}}}\right). \quad (8)$$

The boron diffusion coefficient ($D_{\mathrm{Fe_2B}}$) in the Fe_2B layer in the absence of chemical stress can be estimated numerically by the Newton-Raphson method.

2.2. Chemical stresses generated by boron diffusion in the Fe_2B layer

The derivation of the stress distribution arising from the mass transfer is similar to that arising from heat transfer. The strain-stress relationship can be expressed as follows [17]:

$$\varepsilon_{ij} = \frac{1}{E}\left((1+\nu)\,\sigma_{ij} - \nu\,\sigma_{kk}\delta_{ij}\right), \quad (9)$$

where ε_{ij} is the strain tensor, σ_{ij} are the components of the stress tensor, δ_{ij} is the Kronecker delta, and E and ν are Young's modulus and Poisson's ratio of the Fe_2B layer, respectively. If both the y and z directions are constrained not to vary, their dimensions will be completely suppressed by the application of stresses σ_{yy} and σ_{zz} obtained from Eq. (9), where $\varepsilon_{yy} = \varepsilon_{zz} = -\overline{V}C_{\mathrm{Fe_2B}}[x(t),t]/3$ and $\sigma_{xx} = 0$, or $\sigma_{yy} = \sigma_{zz} = -\overline{V}C_{\mathrm{Fe_2B}}[x(t),t]\,E/3(1-\nu)$ [12]. $\overline{V}$ is the partial molar volume of boron ($1.01\times10^{-5}\,\mathrm{m^3\,mol^{-1}}$), and it is assumed to be constant in the boriding temperature range [18]. The stresses σ_{yy} and σ_{zz} produce axial forces and moments in both the y and z directions. Li [12] and Timoshenko et al. [17] have derived an expression for the stresses in a layer thickness bounded by $x\,(t) = 0$ and $x(t) = u$ when the temperature distribution is independent of the y and z directions. Analogously, the stresses developed in the Fe_2B layer thickness (Fig. 2) by boron diffusion are represented by the following:

$$\sigma_{yy} = \sigma_{zz} = -\frac{\overline{V}C_{\mathrm{Fe_2B}}[x(t),t]E}{3(1-\nu)} +$$

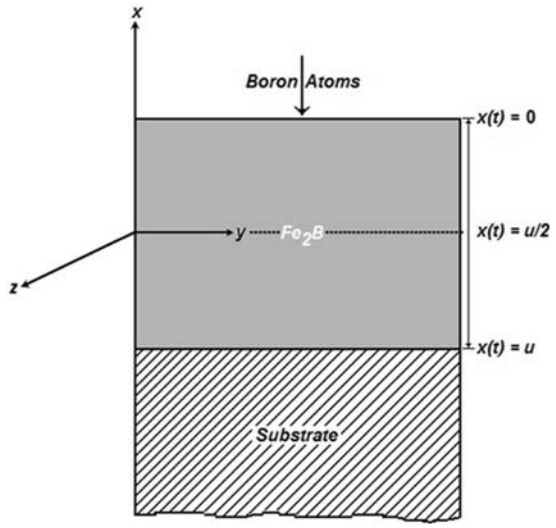

Fig. 2. Schematic diagram of the cross sectional view of Fe_2B layer thickness whose surface is $x(t) = 0$ and interface is $x(t) = u$.

$$+\frac{1}{6u(1-\nu)}\int_{-u}^{u}\overline{V}C_{Fe_2B}[x(t),t]E\,dx+$$
$$+\frac{x}{2u^3(1-\nu)}\int_{-u}^{u}\overline{V}C_{Fe_2B}[x(t),t]Ex\,dx. \quad (10)$$

The first term in Eq. (10) is the contribution of compressive stresses in the layer. As stated by Somers and Christiansen [19], a compressive stress has a pressure effect on the diffusion coefficient, and provides an extra driving force that increases the diffusion depths of solute atoms. The second term is the contribution of tensile stresses, and the third term is the contribution of both stresses in the Fe_2B layer. Substituting the expression for the boron concentration of the Fe_2B layer (Eq. (6)) into Eq. (10), the following transverse stress distribution (σ_t) can be calculated at time $t > t_0(T)$:

$$\sigma_t = -\frac{\overline{V}C_{Fe_2B}[x(t),t]E}{3(1-\nu)}+\frac{\overline{V}C_{up}^{Fe_2B}E}{3(1-\nu)}+$$
$$+\frac{\overline{V}xEB}{4u^3(1-\nu)}\left[\left(2u^2-4D_{Fe_2B}t\right)\mathrm{erf}\left(\frac{u}{\sqrt{4D_{Fe_2B}t}}\right)+\right.$$
$$\left.+4u\sqrt{\frac{D_{Fe_2B}t}{\pi}}\exp\left(-u^2/4D_{Fe_2B}t\right)\right], \quad (11)$$

where $B=\dfrac{C_{low}^{Fe_2B}-C_{up}^{Fe_2B}}{\mathrm{erf}\left(\dfrac{u}{\sqrt{4D_{Fe_2B}t}}\right)}$.

Young's modulus and Poisson's ratio of the Fe_2B layer have mean values of 290 GPa and 0.3, respectively, which were obtained from [20].

2.3. Estimating the effective boron diffusion coefficient in the Fe_2B layer

The driving force of the mass transfer is the gradient of the chemical potential, μ_{Fe_2B}. Using the principle of thermodynamic equilibrium, the chemical potential in an ideal solid solution can be written as the following [13, 21]:

$$\mu_{Fe_2B} = \mu_{Fe_2B}^0 + RT\ln C_{Fe_2B}[x(t),t] - \sigma_h\overline{V}, \quad (12)$$

where $\mu_{Fe_2B}^0$ is the standard-state chemical potential, R is the universal gas constant, T is the absolute temperature, and σ_h is the hydrostatic stress. The hydrostatic stress is one-third of the sum of three normal components, i.e., $\sigma_h = 2\sigma_t/3$. From Eq. (12),

$$\mu_{Fe_2B} = \mu^0 + RT\ln C_{Fe_2B}[x(t),t] - 2\sigma_t\overline{V}/3. \quad (13)$$

Likewise, the diffusion flux is also proportional to the chemical potential gradient [22]:

$$\boldsymbol{J}_{Fe_2B} = -M_{Fe_2B}C_{Fe_2B}[x(t),t]\frac{\partial\mu_{Fe_2B}}{\partial x}\boldsymbol{i} =$$
$$-M_{Fe_2B}RT\left(1-\frac{C_{Fe_2B}[x(t),t]\overline{V}}{RT}\frac{\partial\sigma_h}{\partial C_{Fe_2B}[x(t),t]}\right)\cdot$$
$$\cdot\frac{\partial C_{Fe_2B}[x(t),t]}{\partial x}\boldsymbol{i}. \quad (14)$$

M_{Fe_2B} is the mobility of boron in the Fe_2B layer:

$$\boldsymbol{J}_{Fe_2B}=-D_{Fe_2B}\left(1-\frac{C_{Fe_2B}[x(t),t]\overline{V}}{RT}\frac{\partial\sigma_h}{\partial C_{Fe_2B}[x(t),t]}\right)\cdot$$
$$\cdot\frac{\partial C_{Fe_2B}[x(t),t]}{\partial x}\boldsymbol{i}, \quad (15)$$

where $D_{Fe_2B} = M_{Fe_2B}RT$.

From Eq. (15) it follows that:

$$\boldsymbol{J}_{Fe_2B} =$$
$$-D_{Fe_2B}\left(1-\frac{2C_{Fe_2B}[x(t),t]\overline{V}}{3RT}\frac{\partial\sigma_t}{\partial C_{Fe_2B}[x(t),t]}\right)\cdot$$
$$\cdot\frac{\partial C_{Fe_2B}[x(t),t]}{\partial x}\boldsymbol{i}. \quad (16)$$

Substituting Eq. (11) into Eq. (16) yields the following:

$$\boldsymbol{J}_{Fe_2B} = -D_{Fe_2B}\left(1+\frac{2}{9}\frac{\overline{V}^2E}{(1-\nu)RT}C_{Fe_2B}[x(t),t]\right)\cdot$$
$$\cdot\frac{\partial C_{Fe_2B}[x(t),t]}{\partial x}\boldsymbol{i}. \quad (17)$$

Thus, Eq. (17) can be rewritten as follows:

$$\boldsymbol{J}_{\mathrm{Fe_2B}} = -D_{\mathrm{eff}} \frac{\partial C_{\mathrm{Fe_2B}}[x(t),t]}{\partial x} \boldsymbol{i}. \tag{18}$$

The effective boron diffusion coefficient in the Fe_2B layer (D_{eff}) in the x direction is established as follows:

$$D_{\mathrm{eff}} = -D_{\mathrm{Fe_2B}} \left(1 + \frac{2}{9} \frac{\overline{V}^2 E}{(1-\nu)RT} C_{\mathrm{Fe_2B}}[x(t),t] \right). \tag{19}$$

3. Experimental procedure

Square samples of AISI 1018 commercial steel ($8 \times 8 \times 5$ mm^3) were used for the thermochemical treatment. The boriding process was carried out in a conventional furnace under a pure argon atmosphere. Temperatures of 1123, 1173, 1223 and 1273 K for 2, 4, 6 and 8 h for each temperature were selected. Four millimeters of boron carbide paste was applied to cover the samples. At the end of the boriding treatment, each sample was quenched in oil and cross-sectioned by electrical discharge machining. Structural examinations of the borided samples were conducted by X-ray diffraction (XRD) analysis, and optical microscopy survey. The XRD analysis was carried out on borided samples obtained at a temperature of 1273 K after 8 h and 6 h of exposure. D8 FOCUS equipment was used with Cu Kα radiation at $\lambda = 1.54$ Å. The metallographic preparation employed a sequence of abrasions to 1000-grit silicon carbide abrasion paper, followed by polishing with a diamond paste and ethylene glycol. The thicknesses of the boride layers were measured with GX51 Olympus equipment in a clear field at 200× magnification. The obtained images were analyzed using MSQ PLUS software. For the Fe_2B layer, the penetration depth was determined by selecting needles that reached the deepest into the substrate. In each sample, a minimum of 25 measurements were collected at different points; the reported values are the average layer thicknesses.

4. Results and discussion

4.1. Characterization of boride layers

After the boriding process, the surface of the AISI 1018 steel was covered with a single phase Fe_2B layer with saw-tooth morphology, as shown in Fig. 3. No other phase in addition to Fe_2B was detected within the boride layer by XRD analysis (Fig. 4). Because the growth of the saw-toothed boride layer is a controlled diffusion process with a highly anisotropic nature, higher temperatures and/or longer times encouraged the Fe_2B crystals to make contact with adjacent crystals and forced them to retain an acicular shape [23]. Ninham and Hutchings [24] suggested that the columnar nature of the coating interface is caused by dendrite "side arm" growth similar to the growth that occurs during the solidification of many metallic systems. In borided low-carbon steels, the boride may "*break through*" the band of impurities in some places, which allows local rapid boride growth and results in the characteristic saw-toothed interface. A different mechanism has also been proposed in which local high stress fields and lattice distortions near the tips of the first acicular nuclei of the reaction products are assumed to be responsible for the columnar growth of borides [25]. Boron has been reported to diffuse most rapidly along the [001] direction because of the tendency of boride crystals to grow along the direction of minimum resistance [26].

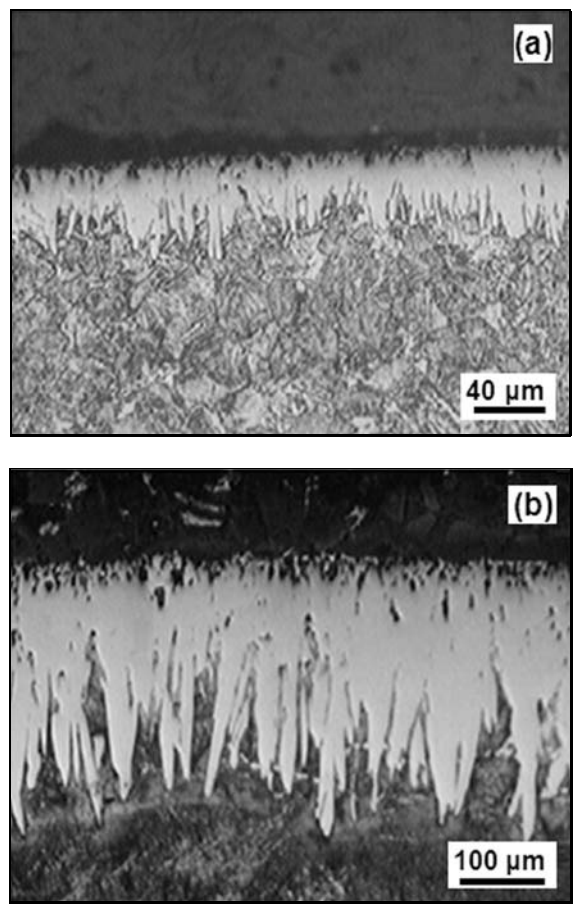

Fig. 3. Saw-tooth morphology of Fe_2B layer formed at the surface of AISI 1018 steel with (a) 2 h of exposure time at a temperature of 1123 K and (b) exposure time of 8 h with a temperature of 1273 K.

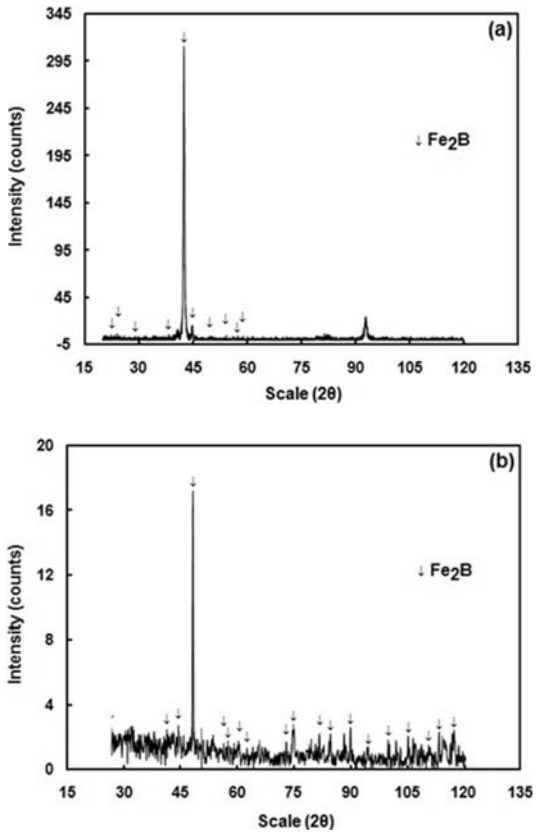

Fig. 4. XRD patterns obtained from AISI 1018 steels borided at a temperature of 1273 K for (a) 6 h and (b) 8 h.

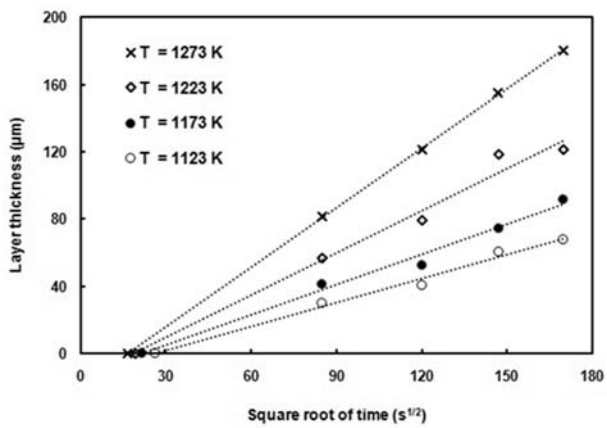

Fig. 5. Growth kinetics of Fe_2B layers at the surface of AISI 1018 borided steel.

4.2. Determining the effective boron diffusion coefficient in the Fe_2B layer

The Fe_2B layers follow a parabolic growth law, $x(t) = u = k_{Fe_2B}\left(t^{1/2} - t_0^{1/2}(T)\right)$, which is depicted in Fig. 5. The incubation time is an additional point in the graph, and the slopes of the straight lines represent the parabolic growth constant k_{Fe_2B}. In general, higher boriding temperatures result in shorter boride incubation times. The effective boron diffusion coefficient in the Fe_2B layer (D_{eff}) with the contribution of chemical stresses was estimated by combining the results obtained from Eq. (8) and Eq. (19). D_{eff} was expressed as a function of the boriding temperature (1123 K to 1273 K) according to the Arrhenius relationship, as follows:

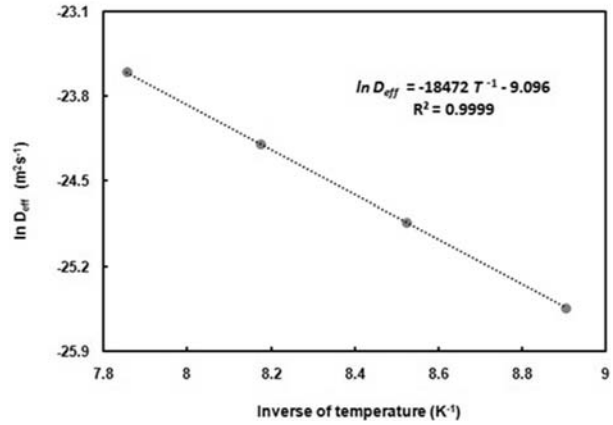

Fig. 6. Behavior of the effective boron diffusion coefficient in the Fe_2B layer as a function of boriding temperature.

$$D_{\text{eff}} = 1.12113 \times 10^{-4} \exp\left(-\frac{153576.208\ \text{J mol}^{-1}}{RT}\right) \left(\text{m}^2\,\text{s}^{-1}\right), \quad (20)$$

where the activation energy value Q, obtained from the slope of the straight line of Fig. 6, represents the energy needed to stimulate the diffusion of boron in the [001] direction along the Fe_2B layer. Table 1 shows the activation energy from [27]. It is important to recall that the model used in the literature does not consider the effect of the boride incubation time and chemical stress in the kinetics of the Fe_2B layer. Furthermore, in [27], the kinetics of the boride layer is extrapolated to $t = 0$, which indicates that boride tends to form instantaneously.

4.3. Comparison of the Fe_2B layer thicknesses obtained by different diffusion models

The mass balance equation proposed in this work (Eq. (8)) has been verified by estimating the Fe_2B layer thickness as a function of temperature and exposure time. For this purpose, a set of boriding conditions in the AISI 1018 steel was examined at temperatures of 1123, 1173, 1223 and 1273 K for 5 h of exposure with a constant 4-mm-thick layer of boron carbide paste over the material surface.

Table 1. Comparison between activation energy values obtained from borided low-carbon steels

Material	Method of boriding	Phases in boride layer	Morphology of the boride layer	Activation energy (kJ mol^{-1})	Reference
AISI 1010	Powder pack	FeB, Fe_2B	Saw-tooth	108	[27]
AISI 1020				110.3	
AISI 1040				118.8	
AISI 1060				124.7	
AISI 1018	Paste	Fe_2B	Saw-tooth	153	This study

Table 2. Empirical equations used in the estimation of the Fe_2B layer thickness

Equations	Formulas
Paraboloid	$u(t,T) = 2425.579936 + 6.389721 \times 10^{-3}t - 4.518107 \times 10^{-3}T - 9.407617 \times 10^{-8}t^2 + 2.80501 \times 10^{-3}T^2$, $(R^2 = 0.9266)$
Gaussian	$u(t,T) = 1891012.714491 \exp\left\{-\frac{1}{2}\left[\left(\frac{t - 27075.533772}{14693.190323}\right)^2 + \left(\frac{T - 4060.32980}{645.494869}\right)^2\right]\right\}$, $(R^2 = 0.9724)$
Lorentzian	$u(t,T) = \frac{527.412409}{\left[1 + \left(\frac{t - 25795.442022}{15249.137240}\right)^2\right]\left[1 + \left(\frac{T - 1443.739788}{119.145325}\right)^2\right]}$, $(R^2 = 0.9476)$
From Equation (21)	$u(t,T) = 2\lambda\sqrt{\frac{D_{Fe_2B}}{\pi}}\frac{t^{1/2}\{1 - [\eta(T)]^{1/2}\}}{\operatorname{erf}\left\{\frac{\varepsilon(T)\{1 - [\eta(T)]^{1/2}\}}{\sqrt{4D_{Fe_2B}}}\right\}}\exp\left(-\frac{[\varepsilon(T)]^2\{1 - [\eta(T)]^{1/2}\}^2}{4D_{Fe_2B}}\right)$ with $\lambda = C_{up}^{Fe_2B} - C_{low}^{Fe_2B}/C_{low}^{Fe_2B} - \beta C_0$

t = exposure time (s), T = boriding temperature (K). The constants of each equation are obtained from the boriding conditions.

Table 3. Experimental and predicted values of the Fe_2B layer thickness for 5 h of exposure at temperatures of 1123, 1173, 1223 and 1273 K

Equations	Temperature (K)			
	1123	1173	1223	1273
	Predicted Fe_2B layer thicknesses (μm)			
Paraboloid	60.06	72.99	96.33	130.08
Gaussian	49.81	70.65	99.61	139.60
Lorentzian	50.70	67.84	94.34	136.93
From Equation (21)	45.86	67.11	95.08	129.03
Experimental Fe_2B layer thickness	48.2	69.6	84.5	129.31

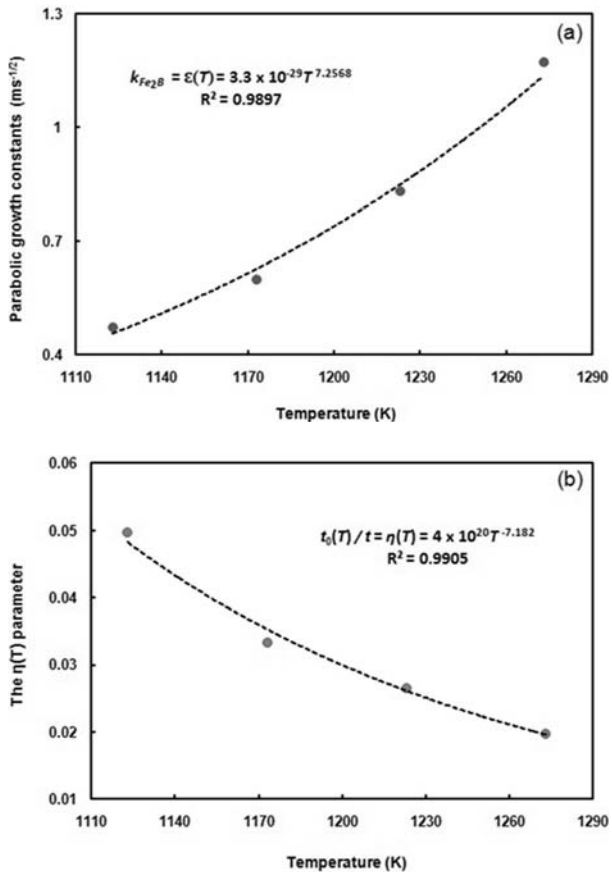

Fig. 7. (a) The growth constant as a function of process temperature, (b) evolution of the $\eta(T)$ parameter as a function of boriding temperature.

According to Eq. (8), the Fe_2B layer thickness, u, can be described as follows:

$$u(t,T) = 2\sqrt{\frac{D_{Fe_2B}}{\pi}}\left(\frac{C_{up}^{Fe_2B} - C_{low}^{Fe_2B}}{C_{low}^{Fe_2B} - \beta C_0}\right) \cdot \frac{t^{1/2}\{1-[\eta(T)]^{1/2}\}}{\operatorname{erf}\left\{\dfrac{\varepsilon(T)\{1-[\eta(T)]^{1/2}\}}{\sqrt{4D_{Fe_2B}}}\right\}} \cdot \exp\left(-\frac{[\varepsilon(T)]^2\{1-[\eta(T)]^{1/2}\}^2}{4D_{Fe_2B}}\right), \quad (21)$$

where $\varepsilon(T)$ is the behavior of the growth constant as a function of the temperature, $k_{Fe_2B} = \varepsilon(T) = 3.3 \times 10^{-29} T^{7.2568}$ (Fig. 7a). In addition, $t_0(T)/t$ is represented by $\eta(T)$, which depends only on the boriding temperature, as shown in Fig. 7b.

Sen et al. [28] proposed several empirical equations (i.e., Paraboloid, Gaussian and Lorentzian equations) to determine the total boride layer thickness (FeB + Fe_2B) depending on the exposure time and boriding temperature in different borided steels. The equations presented in Table 2 were adjusted to the experimental Fe_2B layer thicknesses in the temperature range from 1123 to 1273 K with 2, 4, 6 and 8 h of exposure that were obtained by the boriding of AISI 1018 steels. These expressions were used to estimate the Fe_2B layer thickness after 5 h of exposure to the different boriding temperatures. The results obtained from Eq. (21) show good agreement with the experimental data and the empirical equations depicted in Table 3.

5. Conclusions

Given the theory of elasticity and the diffusion flux equation, a diffusion model is developed to estimate the formation speed of the Fe_2B layers at the surface of AISI 1018 borided steels with the presence of diffusion-induced (chemical) stresses. Therefore, the model can be extended to estimate the growth kinetics of FeB/Fe_2B layers in different borided steels. Moreover, an expression that determines the Fe_2B layer thickness at the surface of AISI 1018 borided steels was generated that takes into account the kinetic parameters of the boriding process. The estimation of the theoretical values of the Fe_2B layer thicknesses formed at 5 h of exposure showed good agreement with the experimental data over the range of boriding temperatures, and with the values estimated with empirical equations proposed in the literature.

Acknowledgements

This work was supported by research grant 150556 from the National Council of Science and Technology in Mexico. I. Campos-Silva thanks the project 20110148 chair supported by the Secretaría de Investigación y Posgrado of the Instituto Politécnico Nacional.

References

[1] DAVIS, J. R.: Surface Hardening of Steels: Understanding the Basics. Ohio, ASM International 2002.
[2] CAMPOS, I.—BAUTISTA, O.—RAMÍREZ, G.—ISLAS, M.—de la PARRA, J.—ZUÑIGA, L.: Appl. Surf. Sci., *243*, 2005, p. 431. http://dx.doi.org/10.1016/j.apsusc.2004.09.099
[3] Graf von MATUSCHKA, A.: Boronizing. Munich, Carl Hanser Verlag 1980.
[4] CAMPOS, I.—OSEGUERA, J.—FIGUEROA, U.—GARCÍA, J. A.—BAUTISTA, O.—KELEMENIS, G.: Mater. Sci. Eng., *A 352*, 2003, p. 261. http://dx.doi.org/10.1016/S0921-5093(02)00910-3
[5] CAMPOS, I.—RAMÍREZ, G.—FIGUEROA, U.—VILLAVELÁZQUEZ, C.: Surf. Eng., *23*, 2007, p. 216. http://dx.doi.org/10.1179/174329407X174416
[6] CAMPOS, I.—ISLAS, M.—GONZALEZ, E.—PONCE, P.—RAMÍREZ, G.: Surf. Coat. Technol., *201*,

2006, p. 2717.
http://dx.doi.org/10.1016/j.surfcoat.2006.05.016
[7] CAMPOS, I.—ISLAS, M.—RAMIREZ, G.—VILLA-VELÁZQUEZ, C.—MOTA, I.: Appl. Surf. Sci., *253*, 2007, p. 6226.
http://dx.doi.org/10.1016/j.apsusc.2007.01.070
[8] KEDDAM, M.: Appl. Surf. Sci., *253*, 2006, p. 757.
http://dx.doi.org/10.1016/j.apsusc.2006.01.011
[9] DYBKOV, V. I.—LENGAUER, W.—GAS, P.: J. Mater. Sci., *41*, 2006, p. 4948.
http://dx.doi.org/10.1007/s10853-006-0032-9
[10] YU, L. G.—CHEN, X. J.—KHOR, K. A.—SUNDARARAJAN, G.: Acta Mater., *53*, 2005, p. 2361.
http://dx.doi.org/10.1016/j.actamat.2005.01.043
[11] BEKE, D. L.—SZABO, I. A.—ERDELYI, Z.—OPPOSITS, G.: Mater. Sci. Eng. A, *387–389*, 2004, p. 4.
http://dx.doi.org/10.1016/j.msea.2004.01.065
[12] LI, J. C. M.: Metall. Trans. A, *9A*, 1978, p. 1353.
[13] CHU, J. L.—LEE, S.: J. Appl. Phys., *75*, 1994, p. 2823.
http://dx.doi.org/10.1063/1.356174
[14] SOMERS, M. A. J.: J. Phys. IV France, *120*, 2004, p. 21.
[15] KIRKALDY, J. S.—YOUNG, D. J.: Diffusion in the Condensed State. London, The Institute of Metals 1987.
[16] CAMPOS-SILVA, I.—ORTIZ-DOMÍNGUEZ, M.—KEDDAM, M.—LÓPEZ-PERRUSQUIA, N.—CARMONA-VARGAS, A.—ELIAS-ESPINOSA, M.: Appl. Surf. Sci., *255*, 2009, p. 9290.
http://dx.doi.org/10.1016/j.apsusc.2009.07.029
[17] TIMOSHENKO, S. P. —GOODIER, J. N.: Theory of Elasticity. New York, McGraw-Hill 1970.
[18] PRUSSIN, S.: J. Appl. Phys., *32*, 1961, p. 1876.
http://link.aip.org/link/doi/10.1063/1.1728256
[19] SOMERS, M. A. J.—CHRISTIANSEN, T.: J. Phase Equilib. Diffus., *26*, 2005, p. 520.
DOI: 10.1361/154770305X66664
[20] FRANTZEVICH, I. N.—VORONOV, F. F.—BAKUTA, S. A.: Elastic Constants and Elastic Modulus for Metals and Non-Metals: Handbook. Kiev, Naukova Dumka Press 1982.
[21] YANG, F.: Mater. Sci. Eng. A, *409*, 2005, p. 153.
http://dx.doi.org/10.1016/j.msea.2005.05.117
[22] CRANK, J.: The Mathematics of Diffusion. United Kingdom, Oxford University Press 1999.
[23] BRAKMAN, C. M.—GOMMERS, A. W. J.—MITTEMEIJER, E. J.: J. Mater. Res., *4*, 1989, p. 1354.
DOI: 10.1557/JMR.1989.1354
[24] NINHAM, A. J.—HUTCHINGS, I. M.: J. Vac. Sci. Technol., *A 4*, 1986, p. 2827.
http://dx.doi.org/10.1116/1.573686
[25] CARBUCICCHIO, M.—BARDANI, L.—SAMBOGNA, G.: J. Mater. Sci., *15*, 1980, p. 1483.
DOI: 10.1007/BF00752129
[26] CAMPOS-SILVA, I.—ORTIZ-DOMÍNGUEZ, M.—CIMENOGLU, H.—ESCOBAR-GALINDO, R.—KEDDAM, M.—ELIAS-ESPINOSA, M.—LÓPEZ--PERRUSQUIA, N.: Surf. Eng., *27*, 2011, p. 189.
[27] CELIK, O.—AYDINBEYLI, N.—GASAN, H.: Prakt. Metallogr., *45*, 2008, p. 334.
[28] SEN, S.—SEN, U.—BINDAL, C.: Surf. Coat. Technol., *191*, 2005, p. 274.
http://dx.doi.org/10.1016/j.surfcoat.2004.03.040